Multipole Interference in the Second-Harmonic Optical Radiation from Gold Nanoparticles

Sami Kujala,* Brian K. Canfield, and Martti Kauranen
Optics Laboratory, Institute of Physics, Tampere University of Technology, PO Box 692, FI-33101 Tampere, Finland

Yuri Svirko and Jari Turunen
Department of Physics and Mathematics, University of Joensuu, P.O. Box 111, FI-80101 Joensuu, Finland
(Received 5 December 2006; published 18 April 2007)

We provide experimental evidence of higher multipole (magnetic dipole and electric quadrupole) radiation in second-harmonic (SH) generation from arrays of metal nanoparticles. Fundamental differences in the radiative properties of electric dipoles and higher multipoles yield opposite interference effects observed in the SH intensities measured in the reflected and transmitted directions. These interference effects clearly depend on the polarization of the fundamental field, directly indicating the importance of multipole effects in the nonlinear response. We estimate that higher multipoles contribute up to 20% of the total emitted SH field amplitude for certain polarization configurations.

DOI: 10.1103/PhysRevLett.98.167403 PACS numbers: 78.67.Bf, 42.25.Ja, 42.65.Ky

Optical responses from metal nanoparticles arise from the plasmonic oscillations of conduction electrons [1]. The plasmon resonances depend on the size and shape of the particles, their dielectric environment, and on their mutual ordering. These resonances can lead to strong local electromagnetic fields in the vicinity of the particles. Such strong local fields may enhance especially the nonlinear optical responses of nanostructures [2–4]. Nanoscale gradients in the local material properties and fields may also enable higher multipoles such as magnetic dipoles, electric quadrupoles, etc. to contribute to the optical responses. However, the precise role of different multipolar orders in the nonlinear responses of nanoscale particles is far from clear.

Usually, the optical responses of particles that are small compared to the wavelength can be described in the framework of electric-dipole approximation. However, when the particle size approaches the wavelength, the dipolar picture may no longer provide a complete description, and higher multipolar interactions should also be considered. When discussing multipoles, it should be noted that there are two types of multipoles: multipoles arising from the light-matter interaction Hamiltonian [5], corresponding to microscopic multipole moments, and multipoles related to Mie scattering theory [1]. Standard Mie theory is based on dipolar interaction, and multipoles arise from the size and retardation effects. However, both microscopic and effective multipoles lead to similar radiation patterns in the far field.

The contribution of multipoles in the linear optical response of metal nanoparticles has been discussed in the literature [6,7]. Krenn *et al.* reported experimental evidence of multipolar plasmon resonances from elongated silver nanoparticles. By changing the nanoparticle length they were able to tailor the optical responses and observed several spectrally separate multipole resonances [8]. Interest in the nonlinear properties of nanoparticles is steadily increasing [9–12]. However, studies concerning the role of multipole contributions in the nonlinear response are scarce.

A first-principles microscopic theory of the nonlinear properties of nanoscale particles is still lacking, although there are several phenomenological treatises [13–17] on the subject of second-harmonic (SH) scattering, where both microscopic multipole moments and nonlinear Mie scattering are included with the result that both contributions are important. Experimental evidence of these effects has been reported [18]. Nappa *et al.* observed strong size-dependent retardation effects in SH scattering from 20–80 nm gold and silver spheres [19,20]. The responses from the smallest particles could be explained using the simple dipole picture, but the responses of larger particles had both dipolar and quadrupolar contributions. The quadrupolar contributions were attributed to retardation effects arising from the nonlocal excitation of surface nonlinearities.

Recently, Klein and co-workers studied second-harmonic generation (SHG) from a metamaterial consisting of split-ring resonators [21]. The SH response was greatest when a magnetic resonance was excited. The response was explained by the fundamental field exciting the magnetic resonance and driving the velocity of electrons, whose coupling through the Lorentz force gave rise to the SH response and led to dipolar radiation. In the suggested mechanism, the magnetic excitation acts as a sort of local field effect. However, the fundamental couplings between the radiated fields and the particles occur through dipolar mechanisms.

In this Letter, we provide experimental evidence that higher multipole radiation accounts for a significant fraction of SHG from arrays of metal nanoparticles. Our experimental method is based on the differences between the fundamental radiative properties of electric dipoles as opposed to magnetic dipoles and electric quadrupoles [22], thereby making the evidence direct. We estimate that for the samples studied, the higher multipoles can contribute

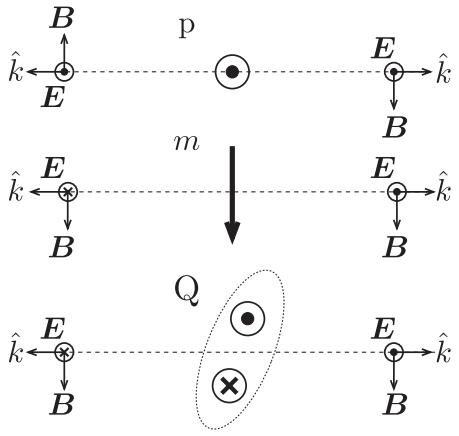

FIG. 1. Simple schematic of the radiative properties of an electric dipole (***p***), magnetic dipole (***m***), and quadrupole (***Q***).

up to 20% of the total emitted second-harmonic field amplitude.

Multipole sources can be recognized by their far-field angular emission patterns. However, in the present work, we measure coherent SH signals, which dominate the response of the surfacelike samples used and give rise to strong signals only in the transmitted and reflected directions. The basis of our measurements is therefore illustrated in a simplified way in Fig. 1, where we compare the radiated far fields of a single electric dipole, a single magnetic dipole, and an effective quadrupole formed from a pair of electric dipoles at a given instant in time. The radiation pattern of a dipole dictates that the direction of the electric field ***E*** does not change when the measurement direction is reversed. However, for both the magnetic dipole and the quadrupole, the direction of ***E*** in the radiated electromagnetic wave does change if we reverse the direction from which we measure the electric field. Therefore, for the case of coherent and directional SHG, the radiative properties of the various multipoles in the transmitted and reflected directions lead to opposing interference effects in the two directions. Moreover, we may expect the strength of the various types of sources to depend on the polarization of the driving field. The response will then exhibit polarization-dependent interference effects, which allows us to distinguish the different multipolar contributions to the overall SHG response, even when the absolute signal levels cannot be calibrated.

In our experiments, we used a sample consisting of an array of L-shaped metal nanoparticles, prepared using electron-beam lithography [23]. The linewidth of the L's is ~100 nm, the arms are ~200 nm long, and the gold layer is 20 nm thick. The nanoparticles are also covered with a 20 nm protective layer of glass. The nanoparticles are arranged in a regular array on a glass substrate, with an array spacing of 400 nm. The period is subwavelength for both the fundamental and SH wavelengths. However, the period is larger than the SH wavelength in the substrate. Therefore, some SH light can be emitted into the substrate, but at such a large angle that it cannot escape the substrate, which leaves only the zeroth diffraction order to contribute to the propagating SH signals. In addition, our technique is not based on absolute signal levels and is therefore not compromised by the emission into the substrate. The active area of the sample is 1×1 mm^2.

The symmetry of an ideal L suggests a set of in-plane coordinate axes, where the x axis coincides with the only in-plane mirror symmetry axis that bisects the arms of the L (cf. Fig. 2). The sample exhibits strong dichroism [24], with the x and y polarizations having well-defined plasmonic resonances at the wavelengths of ~1050 nm and ~1500 nm, respectively. Note that x polarization is near resonant with our laser wavelength, 1060 nm.

Our experimental setup is shown schematically in Fig. 2. A train of femtosecond pulses from a Nd:glass laser system (Time-Bandwith Products GLX-200; 200 fs pulse duration, 350 mW average power, 82 MHz repetition rate) is chopped with an optical chopper and weakly focused

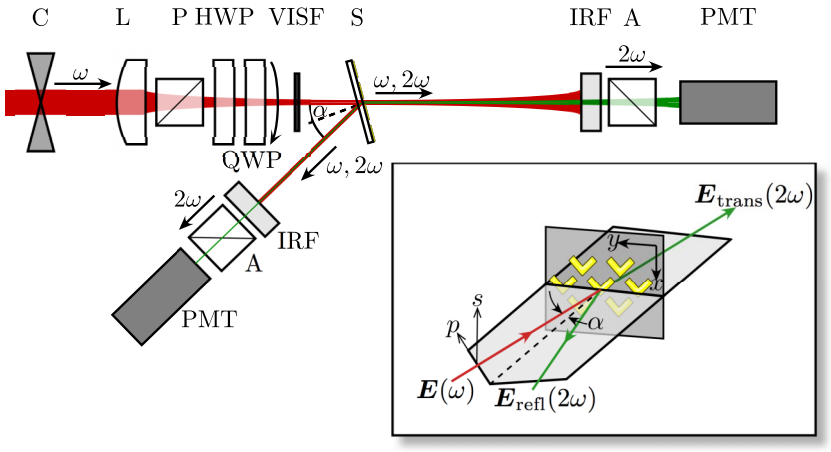

FIG. 2 (color online). Experimental setup. C = optical chopper; L = lens, f = 300 mm; P = polarizer; HWP = half wave plate; QWP = quarter wave plate; VISF = long-wavelength pass filter; S = the sample; IRF = short-wavelength pass filter; A = analyzer; PMT = photo-multiplier tube. Inset: the experimental geometry.

onto the sample with a spot size of ~200 μm. The state of polarization of the fundamental beam is controlled with a half wave plate (HWP) and a quarter wave plate (QWP). The HWP is used to set the azimuth angle of the initial linear polarization, and the QWP, mounted in a computer-controlled motorized rotation stage, modulates the polarization state continuously. The inset in Fig. 2 depicts the experimental geometry. The sample is tilted slightly off normal with respect to the fundamental beam ($\alpha < 2°$) due to experimental constraints in reflection.

The generated SH light is then polarized with an s-directed (normal to the plane of incidence) analyzer. Detecting only s polarization guarantees that differences in transmission and reflection cannot arise from interference between x- and z-directed dipole sources, which would interfere differently for p-polarized (in the plane of incidence) detection [25]. We then detect the s-polarized SH beam as a function of the QWP angle with a sensitive photomultiplier tube connected to a lock-in amplifier referencing the chopper frequency.

The detected polarization line shapes in transmission and reflection are shown in Fig. 3. To analyze the line shape, we fit the data to an equation relating the intensity of the SH signal to the polarization components of the fundamental field [26]:

$$I_{2\omega} = |fE_p^2(\omega) + gE_s^2(\omega) + hE_p(\omega)E_s(\omega)|^2. \quad (1)$$

This model is the most general one, where the complex expansion coefficients f, g, h describe the dependence of the SH response on the various quadratic combinations of the fundamental field. The results of Fig. 3 have been normalized to the maximum intensity in order to accommodate differences in the light collection efficiency of the detection arms for the transmitted and reflected SH beams. This has no influence on the interpretation of our results, because the technique does not rely on absolute signal intensities; rather, only relative differences in the polarization dependence are important.

A significant relative phase shift is immediately apparent between the two data sets. The excellent quality of the fits of the measurement data to Eq. (1) shows that the phase shift is not a measurement artifact, but a real, substantive

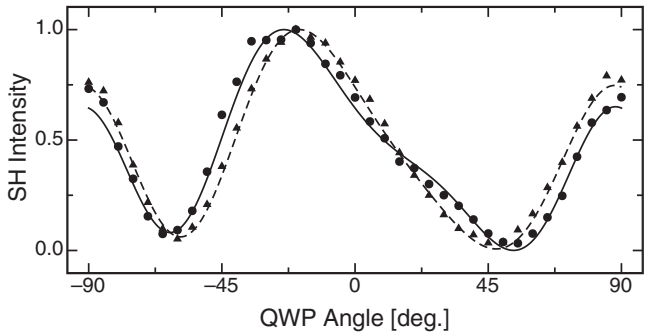

FIG. 3. Measured line shapes. △: transmission SH data; ○: reflection SH data. Solid and dashed lines are fits to Eq. (1) in transmission and reflection geometries, respectively.

effect. The line shapes are very sensitive to small changes in the expansion coefficients and it is therefore impossible to fit, e.g., the transmission line shape using the coefficients from the reflection line shape. This implies that the higher multipolar contributions to the SH response are considerable, but the response is still most likely dominated by a dipole-type response.

To exclude simple alignment issues as explanations of our results, we performed several tests. The influence of the z (normal) component of the fields was checked by repeating the measurements at an incidence angle of approximately 2α. No change in the line shape features was found, implying that the SH response does not couple strongly to the z component for shallow incidence angles. To check the sensitivity of the line shape features to the alignment of the analyzer, the analyzer was tilted $\pm 1°$ away from s polarization. Only a slight decrease in the overall magnitude of the SH intensity was observed. In our previous studies, we have found that similar samples can exhibit optical activity [27]. To rule out the possibility of any polarization effects at the SH wavelength, we used a potassium titanyl phosphate crystal to frequency double the fundamental beam and illuminated the sample with SH light. By comparing the incident and transmitted polarization states, it was found that the sample negligibly alters the state of polarization at the SH wavelength.

Because the angle of incidence is small and the results do not depend on the z component of the fields, the s and p polarizations are essentially equivalent to x and y polarizations. The expansion coefficients f, g, h can then be interpreted as the components of the macroscopic nonlinear response tensor [28] A_{xyy}, A_{xxx}, and $A_{xxy} = A_{yxx}$, respectively. This tensor obeys the electric-dipole-type selection rules for a given experimental geometry, i.e., for reflected and transmitted directions separately. To analyze the results further, we assume that the largest coefficient $g = A_{xxx}$, which is allowed for the ideal symmetry of the structure and is resonant at the fundamental wavelength, is predominantly of electric-dipole origin and normalize it to unity for both directions. The differences in the other two coefficients for the transmitted and reflected directions can then be taken as the measure of the importance of higher multipole contributions. More precisely, we assume that the g coefficient is of purely dipolar origin and radiates symmetrically in the reflected and transmitted directions, while $f = A_{xyy}$ and $h = A_{xxy}$ each consist of two parts:

$$A_{xyy} = A^{s}_{xyy} \pm A^{as}_{xyy}, \quad (2)$$

TABLE I. Results of the fits to Eq. (1)

	Transmission	Reflection	$\lvert A^s \rvert$	$\lvert A^{as} \rvert$
A_{xyy}	$0.66 - 0.58i$	$0.37 - 0.67i$	0.81	0.15
A_{xxx}	1.00	1.00	1.00	0
A_{xxy}	$0.51 - 0.13i$	$0.37 - 0.26i$	0.48	0.10

$$A_{xxx} = A^{s}_{xxx}, \quad (3)$$

$$A_{xxy} = A^{s}_{xxy} \pm A^{as}_{xxy}, \quad (4)$$

where superscripts "s" and "as" refer to parts that transform symmetrically and antisymmetrically between transmission and reflection. Recalling Fig. 1, the symmetric part is identified as originating from the dipolar response, and the antisymmetric part describes the multipolar contribution to the response. The fitted values of the coefficients and their symmetric and antisymmetric parts are shown in Table I. The antisymmetric parts are approximately 20% of the symmetric parts, indicating that the multipolar processes are indeed a non-negligible portion of the total SH response. Note also that largest relative multipolar part is associated with the coefficient $h = A_{xxy}$, which arises from the chiral symmetry breaking of the actual sample [24].

The above analysis shows that higher multipole and electric-dipole contributions to the coherent SH signal can be separated by comparing emission in the transmitted and reflected directions. We believe that both magnetic and quadrupolar emission are equally likely candidates for the higher multipole contribution. Specifically, the x-polarized signal detected along $\pm z$ directions of the laboratory frame (see Fig. 1) can equally originate from the magnetic dipole $\boldsymbol{m}_y$ oriented along the y direction and/or component Q_{xz} of the electric quadrupole tensor.

In conclusion, we have provided experimental evidence of multipolar interference in the SH response from a regular array of gold nanoparticles. The evidence was obtained by comparing the SH responses in the reflected and transmitted directions as a function of the polarization of the incident fundamental beam. The differences in the polarization dependence were interpreted in terms of the different radiative properties of electric dipoles and higher multipoles in the two directions, leading to opposite interference effects. The higher multipole part was estimated to contribute up to ~20% of the total SH field amplitude, depending on the polarization of the fundamental field. This implies that the SH radiation from gold nanoparticles includes contributions beyond the electric-dipole approximation that selectively interfere with the dipolar response. We believe that the higher multipoles arise from nanoscale gradients in the local fields and material properties. The local fields depend on the plasmonic resonances of the individual particles, their defects, and the interparticle coupling through the array structure. For the present sample the resonances arise mainly from the individual particles, with the array playing a lesser role [10].

This work was supported by the Academy of Finland (No. 102018 and No. 209806). S. K. acknowledges the financial support from the Graduate School of the Tampere University of Technology. We gratefully acknowledge Konstantins Jefimovs for preparing the sample used.

*Electronic address: sami.kujala@tut.fi

[1] U. Kreibig and M. Vollmer, *Optical Properties of Metal Clusters*, Springer Series in Materials Science (Springer, New York, 1995).
[2] T. Y. F. Tsang, Opt. Lett. **21**, 245 (1996).
[3] N. Félidj, J. Aubard, G. Lévi, J. R. Krenn, M. Salerno, G. Schider, B. Lamprecht, A. Leitner, and F. R. Aussenegg, Phys. Rev. B **65**, 075419 (2002).
[4] M. I. Stockman, D. J. Bergman, C. Anceau, S. Brasselet, and J. Zyss, Phys. Rev. Lett. **92**, 057402 (2004).
[5] R. Loudon, *The Quantum Theory of Light* (Oxford University Press, New York, 1983), 2nd ed.
[6] S. J. Oldenburg, G. D. Hale, J. B. Jackson, and N. J. Halas, Appl. Phys. Lett. **75**, 1063 (1999).
[7] K. L. Kelly, E. Coronado, L. L. Zhao, and G. C. Schatz, J. Phys. Chem. B **107**, 668 (2003).
[8] J. Krenn, G. Schider, W. Rechberger, B. Lamprecht, F. Leitner, A. Aussenegg, and J. Weeber, Appl. Phys. Lett. **77**, 3379 (2000).
[9] B. Lamprecht, A. Leitner, and F. Aussenegg, Appl. Phys. B **68**, 419 (1999).
[10] B. K. Canfield, S. Kujala, K. Jefimovs, T. Vallius, J. Turunen, and M. Kauranen, Opt. Express **12**, 5418 (2004).
[11] M. D. McMahon, R. Lopez, R. F. Haglund, Jr., E. A. Ray, and P. H. Bunton, Phys. Rev. B **73**, 041401 (2006).
[12] R. Jin, J. E. Jureller, and N. F. Scherer, Appl. Phys. Lett. **88**, 263111 (2006).
[13] V. L. Brudny, W. L. Mochán, J. A. Maytorena, and B. S. Mendoza, Phys. Status Solidi B **240**, 518 (2003).
[14] C. I. Valencia, E. R. Méndez, and B. S. Mendoza, J. Opt. Soc. Am. B **20**, 2150 (2003).
[15] K. Li, M. I. Stockman, and D. J. Bergman, Phys. Rev. Lett. **91**, 227402 (2003).
[16] J. I. Dadap, J. Shan, K. B. Eisenthal, and T. F. Heinz, Phys. Rev. Lett. **83**, 4045 (1999).
[17] J. I. Dadap, J. Shan, and T. F. Heinz, J. Opt. Soc. Am. B **21**, 1328 (2004).
[18] J. Shan, J. I. Dadap, I. Stiopkin, G. A. Reider, and T. F. Heinz, Phys. Rev. A **73**, 023819 (2006).
[19] J. Nappa, G. Revillod, I. Russier-Antoine, E. Benichou, C. Jonin, and P. F. Brevet, Phys. Rev. B **71**, 165407 (2005).
[20] J. Nappa, I. Russier-Antoine, E. Benichou, C. Jonin, and P.-F. Brevet, Chem. Phys. Lett. **415**, 246 (2005).
[21] M. W. Klein, C. Enkrich, M. Wegener, and S. Linden, Science **313**, 502 (2006).
[22] J. Jackson, *Classical Electrodynamics* (Wiley, New York, 1975), 2nd ed.
[23] H. Tuovinen, M. Kauranen, K. Jefimovs, P. Vahimaa, T. Vallius, J. Turunen, N. V. Tkachenko, and H. Lemmetyinen, J. Nonlinear Opt. Phys. Mater. **11**, 421 (2002).
[24] B. K. Canfield, S. Kujala, K. Laiho, K. Jefimovs, J. Turunen, and M. Kauranen, Opt. Express **14**, 950 (2006).
[25] M. Kauranen, T. Verbiest, J. J. Maki, and A. Persoons, J. Chem. Phys. **101**, 8193 (1994).
[26] M. Kauranen, T. Verbiest, and A. Persoons, J. Mod. Opt. **45**, 403 (1998).
[27] B. K. Canfield, S. Kujala, K. Jefimovs, T. Vallius, J. Turunen, and M. Kauranen, Appl. Phys. Lett. **86**, 183109 (2005).
[28] B. K. Canfield, S. Kujala, K. Jefimovs, Y. Svirko, J. Turunen, and M. Kauranen, J. Opt. A Pure Appl. Opt. **8**, S278 (2006).